

SYNTHESIS, SURFACE AND TEXTURAL CHARACTERIZATION OF Ag DOPED POLYANILINE-SiO₂(Pan-Ag/RHA) NANOCOMPOSITES DERIVED FROM BIOMASS MATERIALS

R. J. RAMALINGAM^{a,*}, H. A. AL-LOHEDAN^a, T. RADHIKA^b

^a*Surfactant Research Chair, Chemistry Department, College of Science, King Saud University, Riyadh 11451, Kingdom of Saudi Arabia.*

^b*Centre for Materials for Electronics Technology (C-MET), Athani, Thrissur-680581, Kerala, India.*

Silver doped polyaniline/silica and polyaniline/silica nanocomposite were prepared nontoxic methodology from naturally available rice husk silica. The synthesized materials were characterized by XRD, TG-DSC, FT-IR, SEM and TEM analysis. The formation of polyaniline in salt form exist in benzenoid and quinoid forms. The thermal analysis shows that Ag doped pani/rice husk ash composite is higher thermal stability compared to bulk pani prepared in this study. The UV-Vis absorption spectra of Ag-Pan/RHA, shows two absorption bands obtained (~250-300 and ~ 400-500) is due to polymer in contact with silver nanoparticles. Ft-Raman results provide the bands at 1426 and 1519 cm⁻¹ are due to the C=N stretching vibrations in quinonoid diimine and in polyaniline, a strong band appears at 1598 cm⁻¹ due to the C-C stretching vibration of the benzenoid-like rings. SEM analysis shows the flaky shape morphology for polyaniline and Ag-polyaniline/silica composite forms the petals of flowers morphologies for silver doped nanocomposite. TEM images are confirming the silver nanoparticle incorporation in polymer matrix. Electrochemical activity test of the prepared materials shows the result of promising activity towards supercapacitor applications.

(Received April 30, 2016; Accepted July 12, 2016)

Keywords: Nanocomposite, Sol-gel processes, Polyaniline, Rice husk silica, Silver nanoparticle

1. Introduction

Polyaniline is one of the most studied conducting polymers for electronic, optical, gas sensors and as corrosion protection due to its tunable conducting property, thermal stability, and unique doping/dedoping and redox properties [1, 2]. However, the poor mechanical properties, insolubility in common solvent and low process ability have some drawbacks. In order to overcome these problems, strategies have been developed such as conventional thermoplastic-electro conductive polymer composites with unique properties [2]. In recent years, the preparation of metal nanoparticle polymer composites with synergistic chemical and physical properties has been studied with great attention [3,4]. It can be synthesized easily through either chemical or electrochemical polymerization methods [5]. However, conventional bulk chemical synthesis produces large amount of irregular particle agglomerates and a small amount of polyaniline nanofiber formation. Chemical polymerization of aniline is conducted using relatively strong oxidants like ammonium peroxydisulfate, ferric permanganate, bichromate or hydrogen peroxide. Synthesis of polyaniline by glucose oxidase was reported to depend on the initial generation of H₂O₂ in a broad pH range [6]. Synthesis of conductive composites of polyaniline and inorganic metal ion doping compounds could provide materials with modified properties [7-9]. Among these inorganic materials, silica (SiO₂) has received great attention due to its unique properties and wide

*Corresponding author: rjothiram@gmail.com

application [10,11]. The incorporation of metal particles in conducting polymers has attracted considerable attention in the last two decades because of its numerous applications such as biosensors, electro catalysis and energy storage [12]. The incorporation of metal nanoparticles could effectively improve the electrical, optical and dielectric properties of the polyaniline composite and these properties are very much sensitive by tuning the quantum properties [13]. Recently, Choudary et al., reported polyaniline-supported recoverable and recyclable Sc, In, Pd, Os, and Rh catalysts for a variety of organic transformations [14]. The polyaniline/Ag nanocomposite synthesised by in-situ chemical polymerization exhibit remarkable improvement of electrical conductivity and dielectric properties compared with pure polyaniline [15]. Huang et al. synthesised nanocomposites of polyaniline combined with Ag/Pt nanoparticles simultaneously [16]. Efficient enzyme bio-electrochemical electrodes could be built by polyaniline and silver nanoparticle stabilized with polyvinyl alcohol [17]. The present study reports a facile route for the synthesis of polyaniline (pan) and its composites with waste biomass like rice husk silica and (pan/RHA) and silver doping on RHA (pan-Ag/RHA). The crystalline and thermal stability are explained by XRD, TGA, and DSC. The surface and textural properties has been analysed by BET and electron microscopy techniques. The organic property and chemical environment of polyaniline and silver doped silica nanocoposite has also been studied by H-NMR and Si-NMR technique.

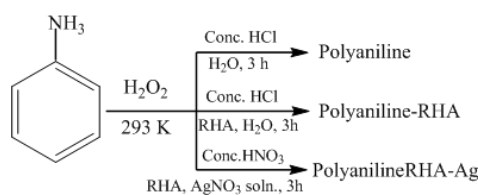
2. Experimental

2.1 Materials Preparation

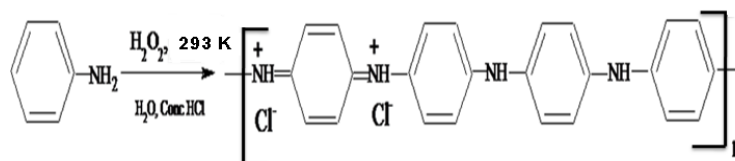
Polyaniline was synthesised by direct oxidation of aniline with hydrogen peroxide. In a typical synthesis, aniline (5.0g, purity 99 %) was dissolved in conc. Hydrochloric acid (15.0 mL, 38.0 %) and it was diluted with distilled water (100 mL) and stirred magnetically for 10 minutes. To this, H_2O_2 (20.0 mL, 30 %) was added and heated initially at 293 K for 10 minutes with continued stirring. The precipitated material of polyaniline was filtered after 3 h, washed with distilled water and followed by washing with acetone and dried at 373 K overnight. The blackish green material thus obtained is collected and labelled as polyaniline.

Rice husk (from a rice mill) was washed and rinsed several times with distilled water in order to remove all the adhered dirt. The washed rice husk (RH) was dried at room temperature and about 30.0 g of the clean RH was stirred in 750 mL of 1.0 M HNO_3 at room temperature for 24 h to remove all metallic impurities. The acid treated RH was washed with distilled water until the pH of the rinse became constant (around 4.6- 5.0), dried in an oven at 373 K for 24 h and kept in a muffle furnace at 873 K for 6 h for complete combustion. The white rice husk ash (RHA) thus obtained was used as source of silica for further material preparation. Polyaniline-silica composite was synthesised by same procedure with addition of 1.0 g of RHA directly into the aniline/conc. HCl mixture. The product was collected after 3h, washed with distilled water followed by washing with acetone and dried at 373 K overnight. The product was labelled as polyaniline-RHA (PanRHA).

For the synthesis of silver doped polyaniline-silica composite, aniline (5.0 g) was dissolved in water (100 mL) and conc. HNO_3 (5.0 mL) and stirred magnetically. The RHA (1.0 g) and 0.1575 g of AgNO_3 , (10 wt.%) were added into this solution and repeated the same procedure with addition of the oxidant, H_2O_2 . Product obtained after 3 h was filtered, washed with distilled water and dried at 373 K overnight. The dark black composite obtained was labelled as Pan-Ag/RHA. Synthesis strategies of polyaniline and polymerization reaction route are given in scheme 1&2.



Scheme 1 Synthesis strategy of polyaniline and it's composite



Scheme 2 Polymerization of aniline using peroxides

2.2 Characterization

The prepared materials were characterized by elemental analysis (Perkin Elmer Series II, 2400), powder X-ray diffraction (Siemens Diffractometer D5000, Kristalloflex operated at 40 kV and 10 mA with nickel filtered $\text{CuK}\alpha$ radiation, $\lambda = 1.54 \text{ \AA}$), N_2 -sorption porosimetry (NOVA 2200e surface area and pore size analyzer, P/P₀ between 0.05 and 0.21) and thermo gravimetric analyses in N_2 atmosphere (TG/DTG 851^e Mettler Toledo). The absorption as well as reflectance spectra were collected on Perkin Elmer Lambda 35 spectrometer in acetonitrile and also with diffuse reflectance technique using KBr pellets as the reference in the range 200–550 nm. FT-IR analysis was carried out on a Perkin-Elmer System 2000 using KBr pellet method. The ^1H NMR spectrum of synthesized polyaniline was recorded in acetonitrile on Perkin spectrometer at 300 KHz. The solid state ^{29}Si and ^{15}N MAS NMR spectra were recorded at 59 MHz on a Bruker DSX 300 spectrometer using TMS and glycine as internal standards respectively. The morphology and elemental loading were observed by SEM (Leica Cambridge S360), (Edax Falcon System) and TEM (Philips CM12). The electrochemical test experiments are carried by three-electrode test cell. Briefly, the as-prepared material, acetylene black and PTFE were mixed in a mass ratio of (80:10:10) Then it dispersed in NMP to produce a homogeneous paste. Then, prepared paste was coated onto the SS substrate grid to fabricate working electrode. Saturated calomel electrode (SCE) was utilized as the reference electrode and Platinum foil was used as the counter electrode.

3. Results and discussion

3.1 Elemental analyses and surface area measurement

The amount of C and N obtained from polyaniline *via* elemental analysis is compared with the element content obtained by EDX analysis. The amount of N was found to be more in polyaniline and it decreased further upon incorporation with silica. In Pani-RHA and Pan-Ag/RHA, the reduction in carbon content suggests successful incorporation of silica into the polymer. The elemental compositions and amount of silicon, silver and chlorine obtained from EDX analysis are shown in Table 1. The presence of chlorine in polyaniline was confirmed from the EDX analysis. Upon silica incorporation the Cl content was decreased. The incorporation of silica and silver in Pan-Ag/RHA was also confirmed by the EDX analysis. The BET surface area of the Pan-Ag/RHA was found to be $87.2 \text{ m}^2/\text{g}$.

Table 1. The element analysis results of Pan and PanRHA-Ag

Material	C (%)		H (%)	N (%)		EDX (%)		
	Elemental analysis	EDX	Elemental analysis	Elemental analysis	EDX	Cl	Si	Ag
Pan	98.10	70.02	-	6.41	7.25	9.05	0	0
PanRHA	19.41	14.81	1.58	2.51	1.48	2.95	36.84	0
Pan-Ag/RHA	14.19	18.37	1.11	1.64	0	0	30.72	1.78

3.2 Powder X-ray diffraction

The wide-angle powder X-ray diffraction pattern of the Pan and Pan-Ag/RHA composites are shown in Fig. 1. In polyaniline, a weak reflection observed at 2θ -value at 25° is characteristic peak of the weak polymer chain. In Pan-Ag/RHA, the sharp peaks centered at $2\theta = 28, 33, 45$ and 77° are assigned to (111), (211), (200) and (311) planes of silver particle exist in the polymer composite. All the peaks can be indexed to the face centered cubic pattern of silver nanoparticles with space group $Fm\bar{3}m$ [4]. Crystallite size of silver calculated by Scherer formula was 12.4 nm. This suggests that the successful incorporation of silver nanoparticles in the polymer composite.

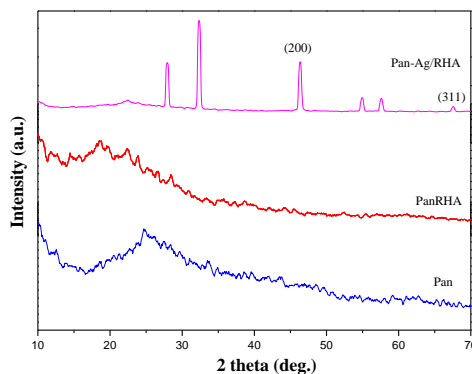


Fig. 1. The powder X-ray diffraction pattern of the materials.

3.3 Thermo gravimetric analysis

The thermal analysis of polyaniline and its composites obtained in N_2 - atmosphere is presented in Fig. 2. The pattern exhibits various mass losses in the region of $100-600^\circ C$. As seen in the pattern, the weight loss below $150^\circ C$ can be ascribed to the removal of loosely bound water molecules and HCl on the surface of the polymer. In polyaniline, the degradation polymer backbone occurs at $300-400^\circ C$ [18]. In PanRHA and Pan-Ag/RHA, the thermograms show higher onset temperatures of degradation due to the presence of more thermally stable silica and silver. This suggests an enhancement in the thermal stability for the prepared polyaniline nanocomposites than that of pure polyaniline.

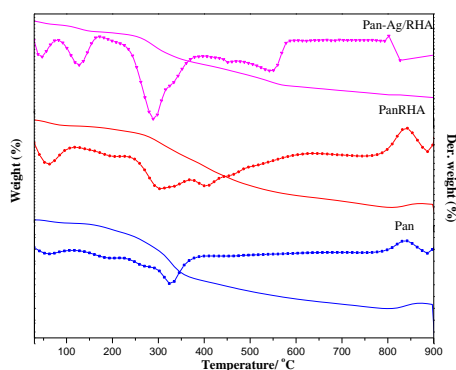


Fig. 2: The TG-DTG analysis of Pan, and Pan-Ag/RHA.

3.4 UV-Vis absorption and DR UV-Vis spectra

The UV-Vis spectrum of polyaniline recorded in acetonitrile is presented in Fig. 3. Two absorption maxima were observed at 260 and 370 nm. The band in the region 240-300 nm is associated with a $\pi-\pi^*$ transitions of the benzenoid rings of polyaniline [19]. The band at 330-450 nm is assigned to the polaron/bipolaron resonance absorption of the electrons [20]. This suggests the formation of the conductive emeraldine salt form of polyaniline by this method in the presence of oxidant. The high intensity of this peak may suggest more conductivity of the polymer composite.

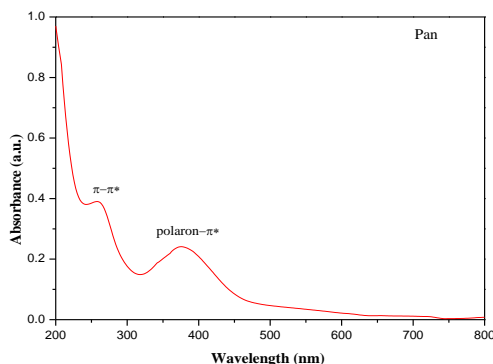


Fig. 3: The UV-Vis spectrum of polyaniline in acetonitrile.

The diffuse reflectance spectra of the prepared materials were obtained with KBr as reference as shown in Fig. 4. The diffuse reflectance UV-Vis spectra of synthesized polyaniline and its composites obtained with KBr pellet shows absorption in the range 250-400 nm with tail extending to higher absorption. Long range absorption of polyanilines suggests more conductivity associated with it. In Pan-Ag/RHA, two absorption bands obtained ($\sim 250-300$ and $\sim 400-500$) and have been distinguished corresponding to polymer in contact with silver nanoparticles.

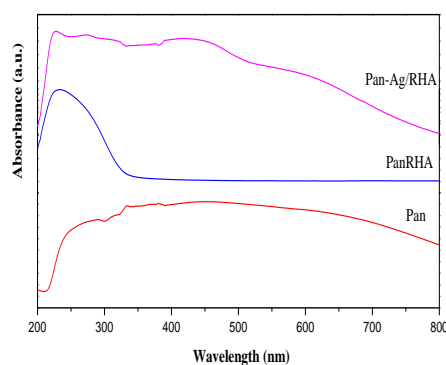


Fig. 4: The diffuse reflectance UV-vis spectra of Pan, PanRHA and Pan-Ag/RHA.

3.5 FT-IR spectral characterization

The FT-IR spectra of polyaniline and other materials are presented in Fig. 5. The molecular structure of synthesized polyaniline and nanocomposite were confirmed by the Fourier transform Infrared (FT-IR) analysis. In all the pattern, the band observed at 1564 cm^{-1} can be assigned to the stretching vibrations of C=N and C=C of the quinoid ring of polyaniline. The bands at 1495 and 1448 cm^{-1} are typical for C=C stretching vibration of benzenoid ring of the polymer. In polyaniline, the bands observed at 1283 and 823 cm^{-1} are due to the C=N stretching of secondary aromatic amine. However, pan-Ag/RHA, the band at 1283 cm^{-1} is not seen or it might be hidden by the large and strong band at 1097 cm^{-1} . This suggest that the possibility of Ag \rightarrow C = N interaction in PanRHA-Ag. In PanRHA and PanAg/RHA, the additional peaks appear at 1097 cm^{-1} corresponds to the vibrations of silica backbone (Si-O-Si) in the polymer. In all the materials synthesized, the O-H and N-H vibrations appear at 3450 and 3231 cm^{-1} , respectively [21].

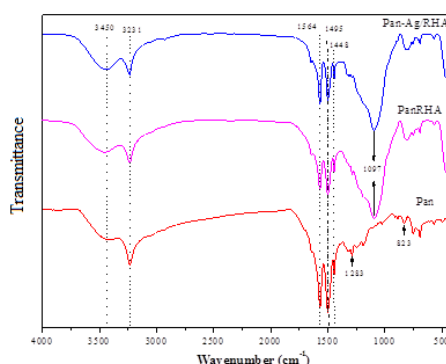


Fig. 5: The FT-IR spectra of Pan, PanRHA and Pan-Ag/RHA.

3.6 FT-Raman spectral characterization

The FT-Raman spectra of polyaniline and its composites are shown in Fig. 6. The band at 1168 cm^{-1} is due to the C-H bending vibrations of benzenoid-like aromatic rings in polyaniline. The decreased intensity of this band in Pan-Ag/RHA suggests progressive oxidation of polymer to form quinoid-like rings. The band at ca. 1239 cm^{-1} can be assigned to the C-N stretching of the secondary aromatic amine (diimine), which is indicative of the emeraldine salt form of polyaniline. The bands at ca. 1393 cm^{-1} is due to the stretching vibrations of C-N⁺ fragments coupled to an aromatic ring and having an intermediate single-to-double bond order. The bands at 1426 and 1519 cm^{-1} are due to the C=N stretching vibrations in quinonoid diimine [22]. In polyaniline, a strong band appears at 1598 cm^{-1} due to the C-C stretching vibration of the benzenoid-like rings indicating that it is less oxidized. The intensity of this band is very much lowered in Pan-Ag/RHA, suggesting a more oxidized form obtained by the present methodology.

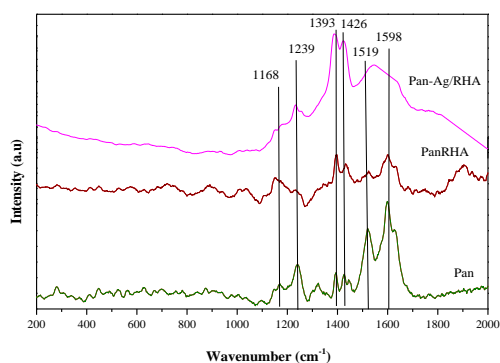


Fig. 6: The FT-RAMAN spectra of Pan, PanRHA and Pan-Ag/RHA.

3.7 The Solid state ^{15}N and ^{29}Si MAS NMR characterization

The ^{15}N is an essential nucleus in the study of polyaniline since it is helpful in determining the structure of the various forms of the polymer. The ^{15}N MAS NMR spectra obtained for polyaniline and the other materials are shown in Fig 7. The shift at ~ 80 - 86 (ppm) can relate to the presence of amine nitrogen ($-\text{NH}-$) in the polymer backbone but with slight change in its chemical shift due to the modification. This change indicates a slightly different chemical environment with the introduction of RHA and Ag. These observations are in accordance to the report of Hopkins et al. [23]. There is however, only one chemical shift for each of the materials. This shows the polymer backbone of the polyaniline did not undergo changes or alterations on incorporating with silica and silver (PanRHA and Pan-Ag/RHA). However, the slight shifting observed is due to the change in the chemical environment around the nitrogen atom resulting upon the incorporation of silica and silver. These observations reinforce the presence of the polymer skeleton as shown in Scheme 2. The ^{29}Si MAS NMR spectra of polyaniline, PanRHA and Pan-Ag/RHA are shown in Fig. 8. The spectra exhibit the ^{29}Si peak at ~ -34 ppm correspond to the Si atom of silica linking with $-\text{CH}$ groups [24]. The absence of T^n signals shows that only physical interaction exists between RHA and polyaniline. The shifting of the ^{29}Si signal on introducing Ag indicates strong interaction between RHA and Ag with a possible interaction with polyaniline.

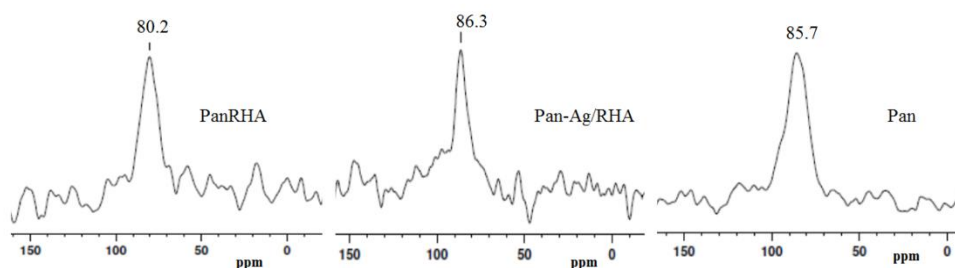


Fig 7: ^{15}N MAS NMR spectra of materials.

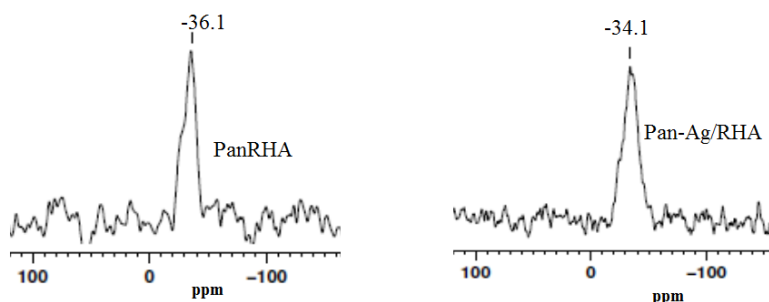


Fig. 8: The ^{29}Si MAS NMR spectra of PanRHA and Pan-Ag/RHA.

3.8 Textural characterization

The scanning electron micrographs of polyaniline and nanocomposites are shown in Fig. 9. The morphology of the prepared polyaniline and its nanocomposites were examined by scanning electron microscopy (SEM). The image of polyaniline appeared as fibrous globules while that of PanRHA as flowers with petals. In Pan-Ag/RHA, it can be seen that the spherical white globules of silver nanoparticles are distributed on the flower petals of the sample. Silver nanoparticle is uniform in size and oriented in a particular fashion for the as prepared sample. The orientation and size of the silver particles may change depending upon the concentration of precursors. Hence, these materials are very interesting towards application in the field of electronic devices. The transmission electron micrographs of polyaniline and nanocomposites are shown in Fig. 10.

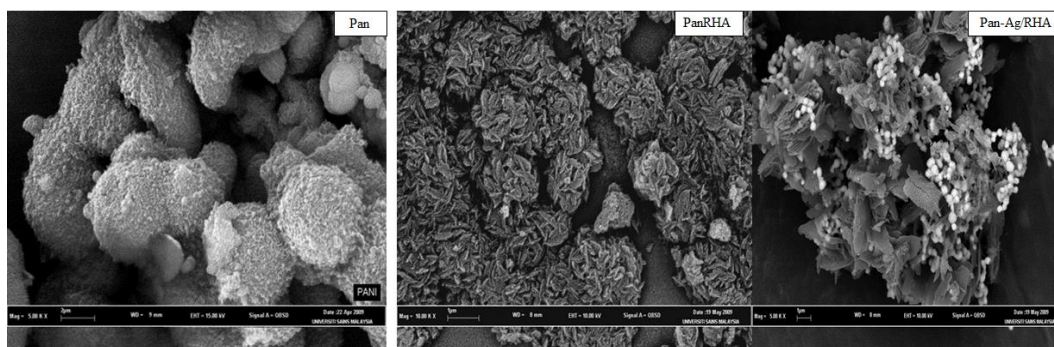


Fig. 9: The Scanning electron micrographs of PanRHA, and Pan-Ag/RHA.

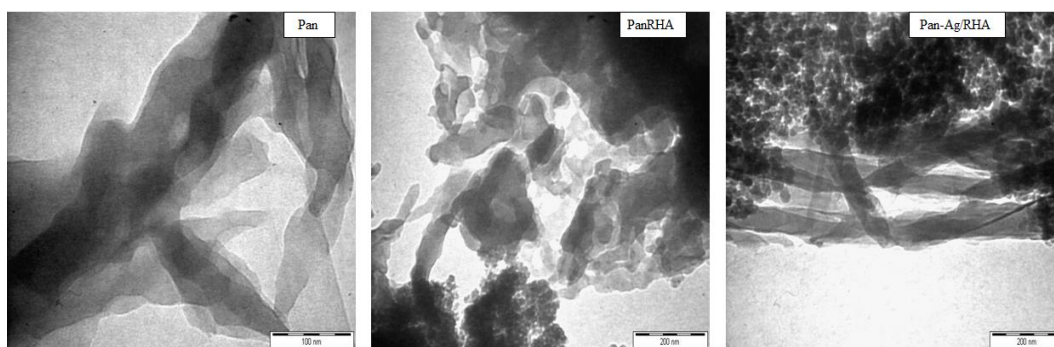


Fig. 10: The transmission electron micrographs of Pan, PanRHA and Pan-Ag/RHA.

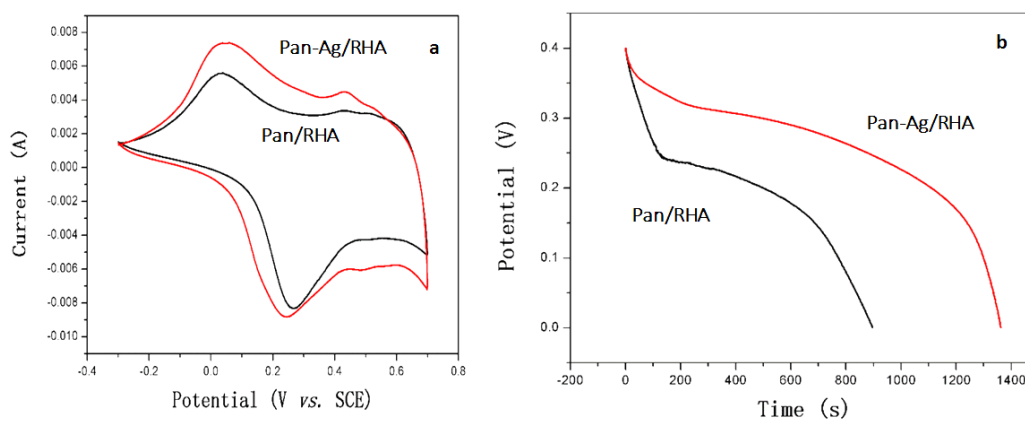


Fig. 11 (a) Cyclic voltammety measurement results of bulk Pan and Pan-Ag/RHA.
(b) Galvanostatic charge/discharge test results of bulk Pan and Pan-Ag/RHA

Fig. 10 depicts the TE micrographs of synthesized polyaniline and its nanocomposites. The image of polyaniline appears as sheaths in which each sheath is of size less than 100nm. PanRHA shows sheaths as well as silica network in nano size. Pan-Ag/RHA shows most of the silver particles are embedded within the thin sheath of the polymer/silica matrix. It is really interesting to observe the sheath like nature of the polyaniline polymer in all three samples. The presence of the sheath like structure confirms the polymeric nature of the samples prepared by this methodology. The electrochemical activity of the as prepared materials are test for preliminary test reactions. Fig. 11a shows the Cyclic voltammetry analysis were carried out to investigate the bulk Pan and pan-Ag/RHA nanocomposite in the voltage range from -0.3 to 0.7 V (vs. SCE), taken at a scan rate of 5 mV/s. A pair of broad and symmetric redox peaks centered at -0.15 V and 0.33 V are appeared due to typical reversible redox reaction of I^-/I_3^- [25]. A similar behaviour is also shown in pan-Ag/RHA, redox peaks centred at 0.15 eV and 0.33 eV, respectively. The peak potential separation (Epp) of bulk and its composite form are calculated and 0.48 eV and 0.18 eV, obtained respectively, demonstrating that the Pan-Ag/RHA has a greater electrochemical activity compared to bulk. Galvanostatic charge/discharge tests were performed to assess the electrochemical capacitance of pan-RAH and Pan-Ag/RHA (Fig. 11b) and its shows clearly that the higher capacitance values achieved at long time for Pan-Ag/RHA compared to pan-RHA. Hence, the prepared low cost composite materials could provide interesting application for super capacitors development.

4. Conclusions

A simple and facile methodology has been developed to prepare polyaniline in emeraldine salt form by oxidative polymerization of aniline using H_2O_2 as an oxidant in acidic media. Thermal analysis suggests that the thermal stability was improved after incorporation of silica and silver particle into polymer matrix. Morphology analysis shows the fiberous nature of polyaniline and polyaniline-silica as flower shaped. In addition, silver nanoparticle in pan/RHA appeared as white globules on the surface of these flower petals. In particular, the prepared nanocomposite exhibited as embedded nanoparticles in the pan-RAH matrix. Hence, it would stimulate the applications of these nanocomposites especially in sensors, catalysis and photo-electronics. The electrochemical activity is further confirms the potential application of as prepared materials towards super capacitor and energy storage applications.

Acknowledgement

This project was financially supported by King Saud University, Vice Deanship of Research Chairs.

References

- [1] D. Zhang, *Polymer Testing* **26**, 9 (2007).
- [2] J. Gao, J.M. Sansiena, H.L. Wang, *Synth. Met.* **135**, 809 (2003).
- [3] G.M. Neelgund, E. Hrehorova, M. Joyce, V. Bliznyuk, *Polym. Int.* **57**, 1083 (2008).
- [4] A. Drury, S. Chaure, M. Kroll, V. Nicolosi, N. Chaure, W.J. Blau. *Chem. Mater.* **19**, 4252 (2007).
- [5] L.G. Jiang, L.H. Peng, *Macromolecules* **40**, 7890 (2007).
- [6] A. Kausaite, A. Ramanaviciene, A. Ramanavicius, *Polymer* **50**, 1846 (2009).
- [7] E. Granot, E. Katz, B. Basnar, I. Willner, *Chem. Mater.*, **17**, 4600 (2005)
- [8] R. Gangopadhyay, D. Amitabha, *Chem. Mater.* **12**, 608 (2000).
- [9] Y. Lee, J. Park, Y. Jun, D. Kim, J. Lee, Y. Kim, S. Oh, *Synth. Met.* **158**, 143 (2008).
- [10] P. Liu, W.M. Liu, Q. Xue *J. Mater. Chem. Phys.* **87**, 109 (2004).
- [11] Y. Wang, X. Wang, J. Li, Z. Mo, X. Zhao, X. Jing, F. Wang, *Adv. Mater.* **13**, 1582 (2001).

- [12] B. Sofiane, H. Didier, L.P. Laurent, *Electrochimica Acta* **52**, 62 (2006).
- [13] T.K. Sarma, D. Choudhury, A. Paul, A. Chattopadhyay, *Chem. Commun.* **14**, 1048 (2002).
- [14] B.M. Choudary, M. Roy, S. Roy, M.L. Kantam, B. Sreedhar, K. Vijay Kumar, *Adv. Synth. Catal.* **348**, 1734 (2006).
- [15] A. Choudhury, *Sensors and Actuators B: Chem.* **138**, 318 (2009).
- [16] L.M. Huang, W.H. Liao, H.C. Ling, T.C. Wen, *Mater. Chem. Phys.* **116**, 474 (2009).
- [17] F.N. Crespilhoa, R.M. Iost, S A. Travainc, O.N. Oliveira Jr., V. Zucolotto, *Biosensors and Bioelectronics* **24**, 3073 (2009).
- [18] R.K. Paul, C.K.S. Pillai, *J. Appl. Polym. Sci.* **84**, 1438 (2002).
- [19] J. Jang, J. Ha and B. Lim, *Chem. Commun.* 1622 (2006).
- [20] Z. Chen, C.D. Pina, E. Falletta, M. Rossi, *J. Catal.* **267**, 93 (2009).
- [21] J. Luo, X. Wang, J. Li, X. Zhao, F. Wang, *Polymer* **48**, 4368 (2007).
- [22] A. Gruger, A.E. Khalki, P. Colomban, *J. Raman Spectroscopy* **34**, 438 (2003).
- [23] A.R. Hopkins, R.A. Lipeles, S.J. Hwang, *Synth. Met.* **158**, 594 (2008).
- [24] S.H. Hosseini, M. Dabiri, M. Ashrafi, *Polym. Int.* **55**, 1081 (2006).
- [25] Y.W. Lee, K. Do, T.H. Lee, S.S. Jeon, W.J. Yoon, C. Kim, J. Ko, S. S. Im, *Synth. Met.* **174**, 6 (2013)